ORIGINAL PAPER

CrossMark

A glassy carbon electrode modified with a composite consisting of gold nanoparticle, reduced graphene oxide and poly(L-arginine) for simultaneous voltammetric determination of dopamine, serotonin and L-tryptophan

Md. Zaved H. Khan[1,2] · Xiaoqiang Liu[1] · Yunfei Tang[1] · Jinhua Zhu[1] · Weiping Hu[1] · Xiuhua Liu[1,3]

Abstract

A glassy carbon electrode (GCE) was modified with poly(L-arginine) (P-Arg), reduced graphene oxide (rGO) and gold nanoparticle (AuNP) to obtain an electrode for simultaneous determination of dopamine (DA), serotonin (5-HT) and L-tryptophan (L-Trp) in the presence of ascorbic acid (AA). The modified GCE was prepared via subsequent 'layer-by-layer' deposition using an electrochemical technique. The surface morphology of the modified electrode was studied by scanning electron microscopy, and electrochemical characterizations were carried out via cyclic voltammetry and electrochemical impedance spectroscopy. The modified electrode showed excellent electrocatalytic activity toward DA, 5-HT and L-Trp at pH 7.0. Figures of merit for the differential pulse voltammetric reponse are as follows: (a) Response to DA is linear in two intervals, viz. 1.0–50 nM and 1.0–50 μM DA concentration range, the typical working voltage is 202 mV (vs. Ag/AgCl), and the detection limit is 1 nM (at an S/N ratio of 3). For 5-HT, the respective data are 10 to 500 nM and 1.0 to 10 μM, 381 mV, and 30 nM. For L-Trp, the respective data are 10–70 nM and 10–100 μM, 719 mV, and 0.1 μM. The modified GCE is fairly selective. It was successfully applied to the simultaneous determination of DA, 5-HT, and L-Trp in spiked urine samples, and high recovery rates were found.

Keywords Electrochemical sensor · Nanocomposite · Cyclic voltammetry · Differential pulse voltammetry · Scanning electron microscopy modified electrode · Urine analysis

Introduction

The neurotransmitters dopamine (DA) and serotonin (5-hydroxytryptamine, or 5-HT) play an important role in the central nervous, cardiovascular, hormonal and renal systems [1–4]. On the other hand, L-tryptophan (L-Trp) is one of the most important essential amino acids having clinical and biochemical significance in humans and herbivores [5, 6]. Due to the coexistence of DA, 5-HT and L-Trp in biological system, their simultaneous determination is an important task. However, the oxidation peaks of these compounds are at a close potential and overlap during simultaneous determination. Moreover, the oxidation potential of ascorbic acid (AA) is very close to that of DA and 5-HT which results in an overlapping voltammetric response.

A great deal of research effort has been directed towards separating the anodic peak of AA, DA, 5-HT, and L-Trp by using different electrochemical techniques [7–9]. Among all analytical methods, electrochemical techniques have been paid much more attention due to high sensitivity, high accuracy and simple operation [10–13]. Poly amino acids modified electrodes have been the focus of intense research interest in the field of electrochemical sensors due to their extraordinary electrocatalytic properties [14, 15]. Among them, poly(L–arginine) has attracted significant attention which can be easily

✉ Xiuhua Liu
ll514527@163.com

1 College of Chemistry and Chemical Engineering, Henan University, Kaifeng 475004, China

2 Department of Chemical Engineering, Jessore University of Science and technology, Jessore 7408, Bangladesh

3 Key Laboratory of Natural Medicine and Immune-Engineering of Henan Province, Kaifeng 475004, Henan, China
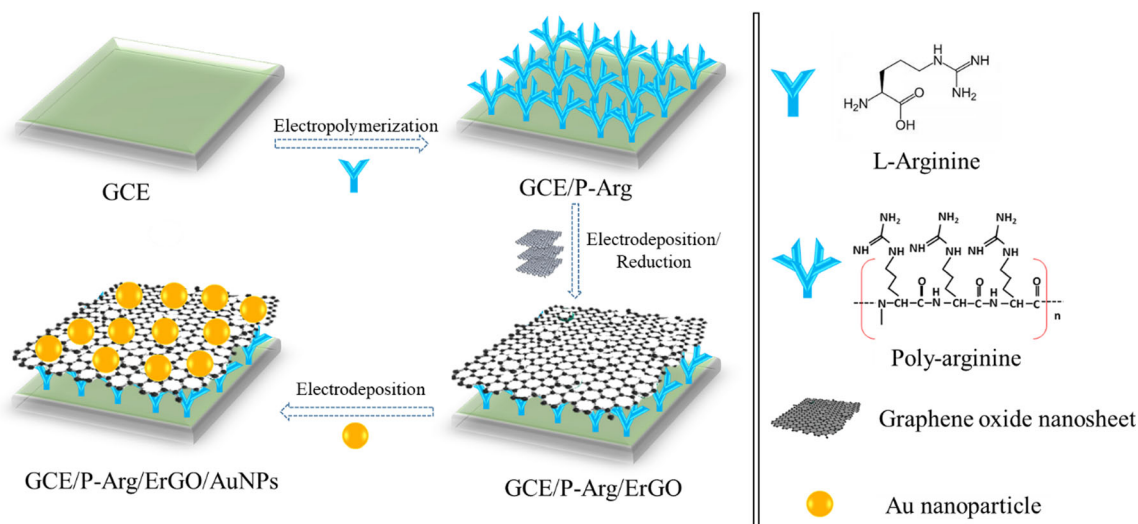
Scheme 1 Step by step modification technique of GCE/P-Arg/ErGO/AuNP modified electrode

electropolymerized on electrode surface through combination of -NH$_2$ and -COOH [16, 17]. Such polymer films can notably improve the stability of the electrode response and improve the electroactivity properties of analytes. For preparing electroactive and functionalized polymers at electrodes surface, electropolymerization is the incredibly convenient method [15].

Few researchers combined polymers and graphene oxide (GO) composites to improve the electrocatalytic performance of the electrodes [15, 18]. The guanidyl group of P-Arg

engaged in hydrogen bonds with unique feature which can electrostatically interact favorably with this partial negative charge groups of GO. Moreover, the free amine group of P-Arg can easily interact with the carboxyl groups of GO. It is well known that GO-based materials provide an effective sensing platform toward the selective detection of bio-entities due to their tunable basal plane oxygen functionalities. The two-dimensional honeycomb sp^2 carbon lattice of reduced graphene oxide (rGO) holds a great potential for sensing applications as it offers a rapid location of redox potentials

Fig. 1 SEM images of bare GCE (**a**), GCE/P-Arg film (**b**), GCE/P-Arg/ErGO film (**c**), and GCE/P-Arg/ErGO/AuNP film (**d**)
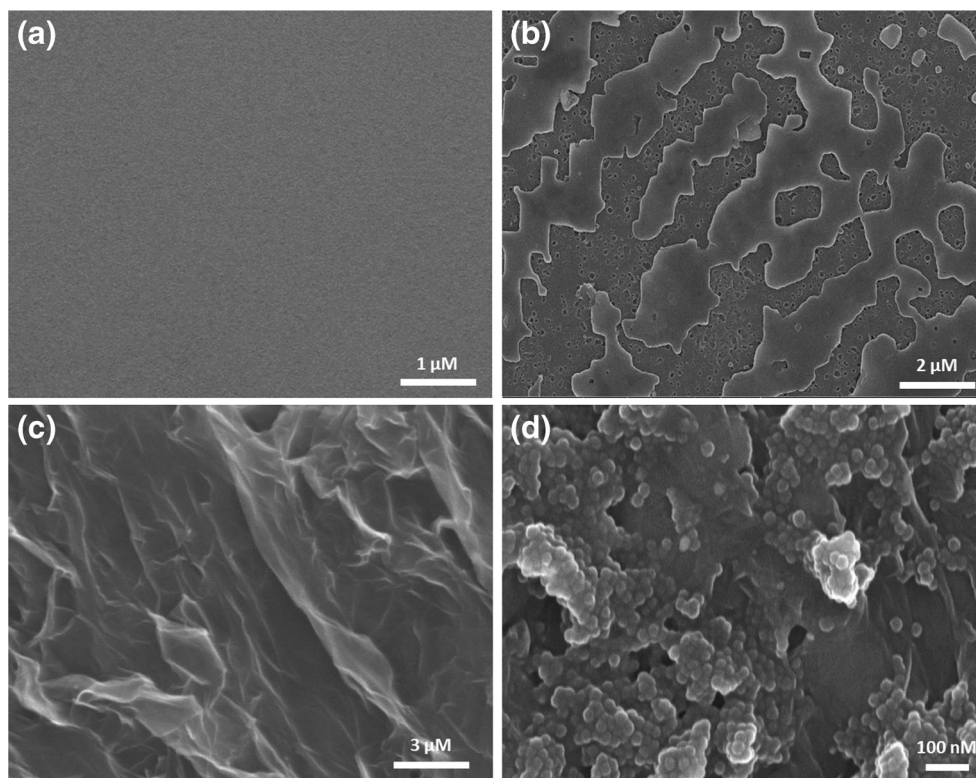
of the electroactive species when employed as an electrode substrate [19, 20]. Preparation of rGO by electrochemical reduction method is recognized as one of the most promising methods that provides highly conductive, low-oxygen-containing graphene sheets without relying on toxic reagents [21, 22].

Moreover, metallic nanoparticles functionalized with rGO have been implemented in different modified electrodes to improve the electrical, thermal, and optical properties of the devices. Among them, Au-nanoparticle (AuNP) decorated graphene oxides are one of the most studied and widely employed in electrochemical sensing, due to the ease of preparation, simple surface functionalization and high analytical sensitivity [23, 24]. Zhang et al. also reported that rGO/AuNP composite shows better catalytic activities than AuNP/GO composite or free AuNP [25].

This work describes a novel electrochemical sensor based on the advantages of poly-Arg, ErGO, AuNP film modified GCE electrode (GCE/P-Arg/ErGO/AuNP) for the simultaneous determination of DA, 5-HT and L-Trp by DPV technique. The formation of 'layer-by-layer' polymer, reduced graphene oxide and metal nanoparticles film was firstly monitored. The electrocatalytic activity of the different modified electrodes was also evaluated. Furthermore, the potential application of the modified electrode for determination of these analytes in the real human urine samples was also investigated.

Materials and methods

Reagents

L-Arginine, dopamine hydrochloride, serotonin hydrochloride, L-Tryptophan, L-Ascorbic acid, Tetrachloroaurate ($HAuCl_4$) trihydrate were purchased from Aladdins Reagent, Shanghai, China (http://www.aladdin-e.com). Modified Hummers method was used to prepare graphene nanosheet from natural graphite powder as described in previous work [26] and it was kindly supplied by Prof. Yuta Nishina, Japan. All the reagents for GO nanosheet preparation were purchased from Sigma Aldrich (http://www.sigmaaldrich.com/). The solutions of AA, DA, UA and L-Trp were prepared daily by dissolving the required amount of reagent in 0.1 M PB (pH 7.0). A redox probe solution was prepared in 0.1 M KCl, which contained 5.0 mM $Fe(CN)_6^{3-}$ and 5.0 mM $Fe(CN)_6^{4-}$.

Preparation of the modified electrode (GCE/P-Arg/ErGO/AuNP)

The sequential 'layer-by-layer' film was fabricated on a GCE with a diameter of 3 mm by cyclic voltammetry (CV). Prior to modification, the GCE electrode was mirror fine-polished

with 0.05 μm alumna slurry on microcloth pads and then subsequently ultrasonically washed using nitric acid (1:1), ethanol, and deionized water. Next, the electrode was rinsed with doubly distilled water and dry under N_2. Scheme 1 illustrates the details of the modification procedure. The cleaned GCE was dipped into 0.1 M PB (pH 7.0) containing 2.5 mM L-Arg and cyclic voltammetry (CV) was performed
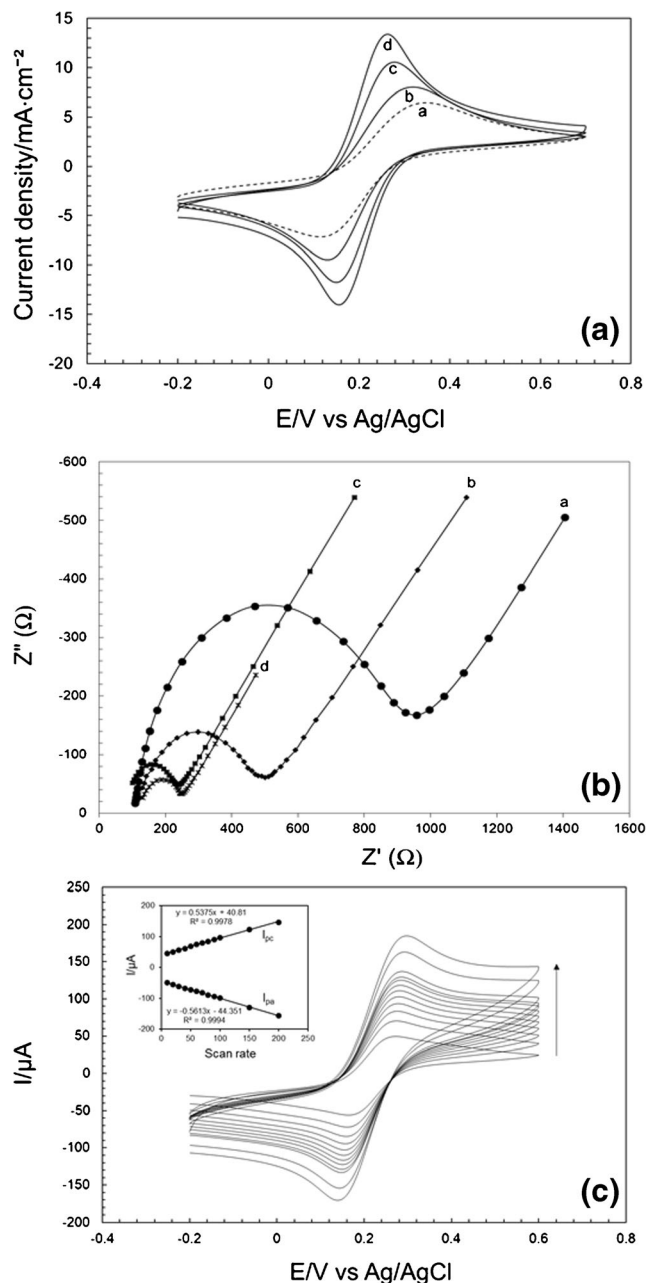

Fig. 2 Cyclic voltammograms (**a**) and Nyquist plot of EIS (**b**) of the different electrodes measured in 0.1 M KCl including 5.0 mM $Fe(CN)_6^{3-/4-}$: (a) bare GCE, (b) GCE/P-Arg, (c) GCE/P-Arg/ErGO, and (d) GCE/P-Arg/ErGO/AuNP. CV response for GCE/P-Arg/ErGO/AuNP at different scan rates (from inner to outer): 10, 20, 30, 40, 50, 60, 70, 80, 90, 100, 150 and 200 mV/s in 0.1 M KCl including 5.0 mM $Fe(CN)_6^{3-/4-}$ solution (**c**). All potentials are given vs. Ag/AgCl. The inset shows the dependence of peak currents on the scan rates

Fig. 3 The CV curves of AA (200 μM), DA (5 μM), 5-HT (10 μM) and L-Trp (10 μM) recorded on bare GCE (a), GCE/P-Arg (b), GCE/P-Arg/ErGO (c), and GCE/P-Arg/ErGO/AuNP (d) in phosphate buffer of pH 7.0, scan rate set at 100 mV s^{-1}
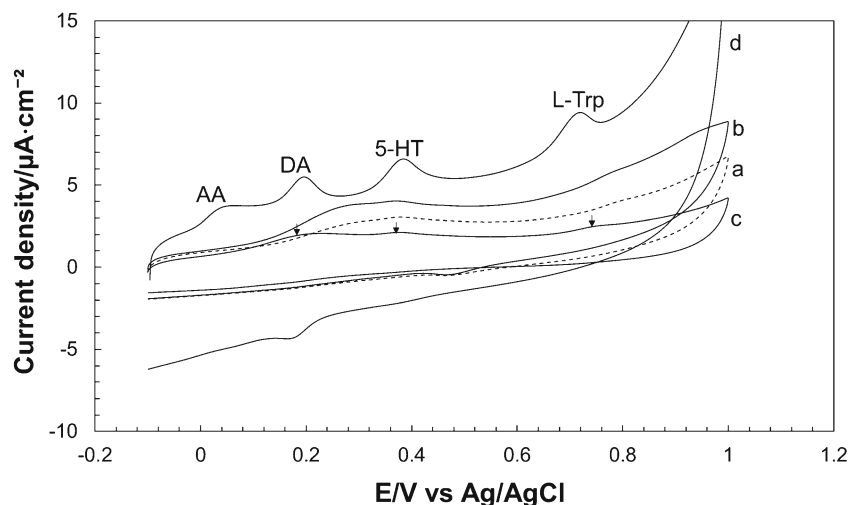
in the potential range from −2.2 to 2.0 V at 100 mV s^{-1} for a defined cycle. After electropolymerization, the GCE/P-Arg electrode was carefully washed with ultrapure water and dried in air. To prepare GCE/P-Arg/ErGO film, 0.5 mg ml^{-1} GO was dispersed in 0.1 M PB (pH 7.0) solution in nanosheet form and was prepared according to our previous report [27]. Later, CV method (condition: 15 cycles @ −1.4 and 0.7 V vs. Ag/AgCl at a scan rate of 50 mVs^{-1}) was used for electrodeposition of GO on GCE/P-Arg electrode under deoxygenated conditions. After electrodeposition, the modified electrode GCE/P-Arg/ErGO was washed with ultra-pure water, and then air-dried. Subsequently, the modified electrode was immersed in 0.5 mM HAuCl$_4$ + 0.1 M KNO$_3$ aqueous solution and CV was run for 20 continuous cycles (−0.5 to 0 V at a scan rate of 50 mVs^{-1}) to obtain GCE/P-Arg/ErGO/AuNP modified electrode. At last, the GCE/P-Arg/ErGO/AuNP was carefully washed with ultra-pure water and stored in 4 °C for use. For electrode characterization and comparison, four different electrodes were also prepared with or without P-Arg, ErGO, and AuNP respectively.
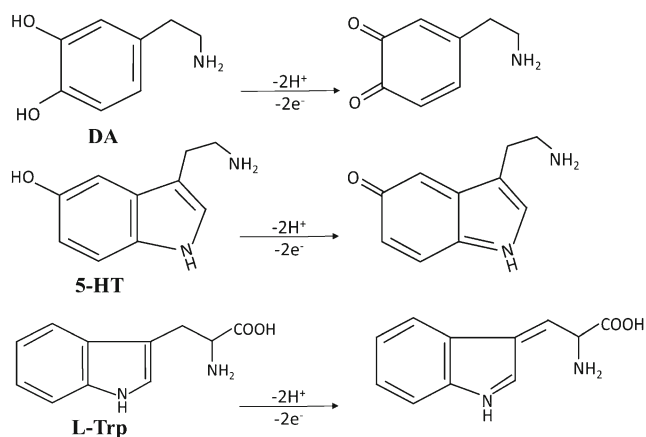
Scheme 2 Electrochemical oxidation of DA, 5-HT, and L-Trp at GCE/P-Arg/ErGO/AuNP modified electrode

Detection of DA, 5-HT and L-Trp in real sample

The sensor was applied to the analysis of real urine samples in order to assess its analytical performance. Following the standard addition method, 0.1 mL of human urine sample was spiked to 10 ml of PB solution (0.1 M, pH 7.0) and purged N$_2$ to removal oxygen. Different concentrations of standard analyte solution were added to the diluted urine samples. We then measured the DPV curves in a potential range of 0.0 V to 1.0 V with amplitude of 50 mV and a pulse width of 0.2 s.

Apparatus

CHI electrochemical workstation (Shanghai CH Instruments, Model CHI-660E) (http://www.chinstruments.com/) with conventional three electrode system was used for electrochemical measurements. Electrochemical impedance spectroscopy (EIS) studies were analyzed using ZAHNER impedance analyzer EIM6ex ZAHNER (Kroanch, Germany) (http://zahner.de/). Before the EIS measurements, the electrode was cycled for 3 cycles and then measured in a frequency range from 0.01 Hz to 1.0 MHz. A small ac signal of 10 mV in amplitude was used as the perturbation of the system throughout the tests. Hitachi S-3000H model (https://www.hitachi-hightech.com) scanning electron microscopy (SEM) was used for surface characterization. All voltammetric measurements were carried out at room temperature under nitrogen (N$_2$) atmosphere.

Results and discussion

Choice of materials

Graphene is an outstanding material which exhibits larger surface area, higher electrical conductivity and better stability

than carbon nanotubes or carbon dots. The combination of graphene oxide and polymer composite enhance the performance of biosensors in terms of sensitivity, selectivity and efficiency. Compared with other polymers, the multidentate characteristics of P-Arg provide electrostatic interactions with negatively charged groups of GO. Owing to low-cost, versatility and easiness of the electrodeposition, P-Arg/ErGo composite has been used for the modification of electrode. In contrast to graphene and GO, reduced graphene oxide ensures high electrochemical activity, more reactive sites, as well as the more efficient charge transport. Moreover, AuNP were employed for improving the analytical sensitivity of the modified electrode.

Characterization of the modified electrode (GCE/P-Arg/ErGO/AuNP)

The details observation of the layer-by-layer electrodeposition process was described in electronic supporting material (ESM) section S1–3. We adopted cyclic voltammetry technique for both electropolymerization and electrodeposition along with AuNP deposition without any reducing agents onto the electrode surface. SEM measurements were done to investigate the surface morphology of the bare and different modified GCE and presented in Fig. 1. The image of Fig. 1b shows the P-Arg layer clearly deposited on GCE with regular and patterned interconnected net-like structure. The observed surface morphology indicates that P-Arg film has been successfully adhered to the electrode surface. After electrochemical deposition/reduction of GO, the ErGO nanosheets were observed as well connected and closely arranged thin folded sheets as shown in Fig. 1c. Finally, AuNP with an average size of ~30 nm uniformly and densely decorated along the surface of ErGO film by electrodeposition at 50 mVs^{-1} (Fig. 1d). The size distribution of AuNP in the electrodeposited GCE/P-Arg/ErGO/AuNP film was presented in Fig. S4. However, the electro-deposited AuNP were slightly aggregated due to the absence of any stabilizing functional groups in ErGO film.

The electrochemical characterization of the bare and modified electrodes was performed via CV and EIS in 0.1 M KCl including 5.0 mM Fe(CN)$_6^{3-/4-}$. A pair of well-defined redox peaks corresponding to Fe(CN)$_6^{3-/4-}$ appeared with the lowest peak currents at the bare GCE. The peak to peak separation (ΔEp) value was calculated as 254 mV for bare GCE electrode which indicates the occurrence of a slow electron-transfer kinetics at the surface of the bare GCE. However, after electrodeposition of L-Arginine, the anodic and cathodic peaks increased with a ΔEp value of 185 mV. As reported by earlier researchers, the electrochemical reaction of Fe(CN)$_6^{3-/4-}$ effectively facilitated by the positive charges of poly(L-arginine) [5, 15]. After electrodeposition of GO, the peak current significantly increased as shown in Fig. 2a, with

a ΔEp value of 123 mV which indicates increased electrochemical active sites with ErGO modification. The highest redox current and lowest potential difference were observed with GCE/P-Arg/ErGO/AuNP modified electrode. The possible reason may be ascribed to that the conductive graphene sheets connected individual AuNP and effectively facilitated electron transfer between the modifying layer and GCE substrate, thus resulting in synergic effect. These observations
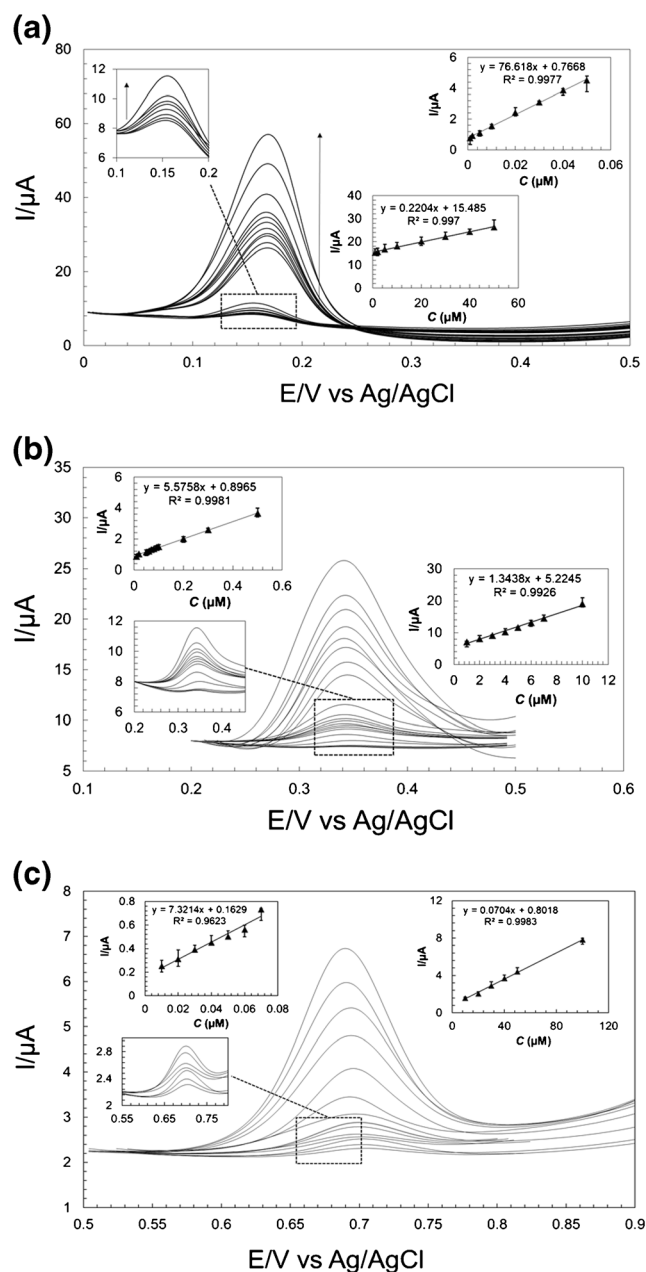
Fig. 4 a DPVs for determination of DA using GCE/P-Arg/ErGO/AuNP electrode in pH 7.0 phosphate buffer at scan rate of 50 mV s^{-1} with a wide range of concentrations from 0.001 to 50 μM of DA; (b) Determinations of 5-HT with a wide range of concentrations from 0.01 to 10 μM; and (c) Determination of L-Trp with a wide range of concentrations from 0.01 to 100 μM. All the inset show the corresponding calibration plots for high and low concentrations ranges

demonstrated excellent electro-catalytic prosperities of the modified GCE/P-Arg/ErGO/AuNP electrode.

We have also calculated the electrochemical active surface area for bare and modified electrodes based on the Randles–Sevcik equation (Eq. 1) [28].

$$I_p = 2.69 \times 10^5 A D^{1/2} \, n^{3/2} \, \gamma^{1/2} C \qquad (1)$$

Where A is the electroactive surface area, C is the concentration of the probe molecule, D is the diffusion coefficient ($6.70 \pm 0.02 \times 10^{-6}$ cm^2/s), γ is the scan rate (V/s), and n is the number of electrons in the redox reaction. The calculated A value for the GCE, GCE/P-Arg, GCE/P-Arg/ErGO, and GCE/P-Arg/ErGO/AuNP were 0.085 cm^2, 0.135 cm^2, 0.204 cm^2 and 0.288 cm^2 respectively. This finding proved that GCE/P-Arg/ErGO/AuNP modified electrode has the maximum electrochemical active surface area and high electron transfer kinetics.

Electrochemical impedance spectroscopy (EIS) experiments were performed to confirm the synergy between various modified electrodes and the results were shown in Fig. 2b. Theoretically, the electron-transfer kinetics of the redox probe at the electrode interface controlled by the charge transfer resistance (R_{ct}) which represents the diameter of the semicircular portion presented in the Nyquist plot at higher frequencies of the EIS. It was observed that the bare GCE shows the largest semicircle. The R_{ct} value of 922 Ω underpins the low transfer rate. Whereas GCE/P-Arg modified electrode shows a R_{ct} value of 379 Ω. The diameter of semicircle obviously decreases after ErGO modification owing to the high electrical conductivity. The smallest semicircle (R_{ct} value of 115 Ω) was observed at the GCE/P-Arg/ErGO/AuNP indicating that the synergistic effect of the conductivity of ErGO and AuNP layer, thereby promoting a higher electron transfer rate in the redox probe.

Moreover, the relationship between different scan rate and peak current was also studied to investigate the electrochemical mechanism of the electrode. From Fig. 2c, it can be observed that the peak currents increased with scan rate (in the range of 10–200 mV/s) for GCE/P-Arg/ErGO/AuNP modified electrode. A linear relationship with good correlation coefficients was observed between the peak current values and the scan rate as shown in the inset of Fig. 2c.

Electrochemical behavior of target analytes at different electrodes

CV behaviors of the bare and modified GCE electrodes were individually investigated in 0.1 M PB (pH 7.0) by adding target analytes. Figure 3 displays the cyclic voltammograms of AA, DA, 5-HT, and L-Trp at the bare GCE (a), GCE/P-Arg (b), GCE/P-Arg/ErGO (c), and GCE/P-Arg/ErGO/AuNP (d), respectively. A broad peak was observed at the bare GCE due to the overlapping oxidation peaks of AA, DA. However, the GCE/P-Arg/ErGO/AuNP electrode successfully separated the voltammetry peaks into four well-separated peaks at the potentials of 0.048 V (AA), 0.202 V (DA), 0.381 V (5-HT) and 0.719 V (L-Trp), which were large enough to determine AA,

Table 1 Comparison of the parameters from the electrochemical detection of DA, 5-HT, and L-Trp with different methods and modified electrodes

| Electrode | Linear range (μM) | | | LOD (μM) | | | |
	DA	5-HT	L-Trp	DA	5-HT	L-Trp	Reference
NiO/CNT/PEDOT/GCE	0.03–20	0.3–35	1–41	0.026	0.063	0.210	[29]
Graphene/CP/SPCs	0.05–100	0.05–150	–	0.002	0.003	–	[11]
CPE-MWCNTs	2.00–170	–	0.60–100	0.36	–	0.065	[30]
NiO–CuO/GR	0.5–20	–	0.3–40	0.17	–	0.1	[31]
Au/CoS$_2$/IL-GN/GCE	0.1–400	–	–	0.04	–	–	[32]
rGO-Mn$_3$O$_4$/Nafion-Au	1–1450	–	–	0.25	–	–	[33]
MWCNT/PSVM/Au/GCE	0.2–1000	–	–	0.056	–	–	[34]
β-CD/CQDs/GCE	4–220	–	5–270	0.14	–	0.16	[35]
MWNTs-SiO$_2$-chitosan	1–20	0.1–2.0	–	0.2	0.01	–	[36]
AgNPs/P(Arg)-GO	0.05–50	–	1.0–150	0.01	–	0.122	[5]
NiCo$_2$O$_4$/Nano-ZSM-5	0.6–900	–	0.9–1000	0.5	–	0.7	[37]
PTh/GPE	10–180		6–180	1.0		0.6	[38]
GCE/P-Arg/ErGO/AuNP	0.001–0.05	0.01–0.5	0.01–0.07	0.001	0.03	0.1	This work
	1.0–50	1.0–10	10–100				

CNT- carbon nanotube; PEDOT-poly(3,4-ethylenedioxythiophene); CP-conducting polymer; SPCs-screen printed carbon sensor; CPE-MWCNTs-carbon paste electrode modified with multi-walled carbon nanotubes; (CPE-MWCNTs); CoS$_2$-cobalt disulfide; IL-ionic liquid; PSVM- poly(vinylbenzyl thymine-co-styrene-co-maleic anhydride); β-CD-poly(β-cyclodextrin); CQDs-carbon quantum dots; Nano-ZSM-5-Nanocrystalline zeolite; PTh-Polythiophene nanostructures; GPE-graphite paste electrode.

DA, 5-HT and L-Trp individually and simultaneously. The separations of E_p of AA–DA, DA–5-HT and 5-HT–L-Trp were of 154, 179 and 338 mV, respectively. These results indicate that the simultaneous detection of DA, 5-HT and L-Trp is feasible with the sensor. The excellent electrochemical performance can be ascribed to the synergistic effects between the ErGO and AuNP that would be beneficial for improved electron transfer kinetics.

Individual voltammetric responses of DA, 5-HT, and L-Trp

The electrochemical oxidation mechanism of target analytes at GCE/P-Arg/ErGO/AuNP modified electrode was illustrated in Scheme 2. The electrochemical behavior of modified electrode in the presence of DA, 5-HT, L-Trp was investigated by differential pulse voltammograms (DPV) in wide potential range. All experimental procedures were performed in 0.1 M PB (pH 7.0) at room temperature. For all the DPV analysis, we have employed the following parameters: constant time interval of 90 s; N_2 gas purging into the electrolyte solution for 5 min before the start of each experiment. Figure 4a, b and c, illustrates the DPVs for the individual detection of DA, 5-HT, and L-Trp and their calibration plots. As shown in Fig. 4a, the change of DPVs indicates that the oxidative peak current (I_{pa}) has linear relationship with the DA concentration. The calibration plot for DA exhibits two linear segments in the range from 1.0 to 50 nM ($R^2 = 0.997$), and 1.0 to 50 μM ($R^2 = 0.997$), with a detection limit (S/$N = 3$) of 1 nM. On the other hand, a linear relation between the concentration of 5-HT and the peak current (Fig. 4b) was in the range of 10 to 500 nM ($R^2 = 0.998$) and 1.0 to 10 μM ($R^2 = 0.992$), with a detection limit of 30 nM (S/N = 3). As shown in Fig. 4c, the peak current of L-Trp increases linearly with its two concentration range from 10 to 70 nM ($R^2 = 0.999$), and 10 to 100 μM ($R^2 = 0.998$), with a detection limit of 0.1 μM (S/N = 3). The sensor has a better ability to determine target analytes over a broader range of concentrations. The observed two linear concentration ranges correspond to low and high concentrations can be attributed to the sensor nature; due to the variation in its analytes concentration tolerance. Same results were verified with repeated tests. The calculated sensitivities for DA, 5-HT, and L-Trp are 2.48 μA·μM^{-1}·cm^{-2}, 5.97 μA·μM^{-1}·cm^{-2}, and 0.35 μA·μM^{-1}·cm^{-2} respectively. Moreover, the analytical findings of this study were compared with several modified electrodes reported in last few years and presented in Table 1.

Repeatability, reproducibility, stability and interference study

A series of repetitive voltammetric measurements were carried out at the same GCE/P-Arg/ErGO/AuNP electrode to evaluate

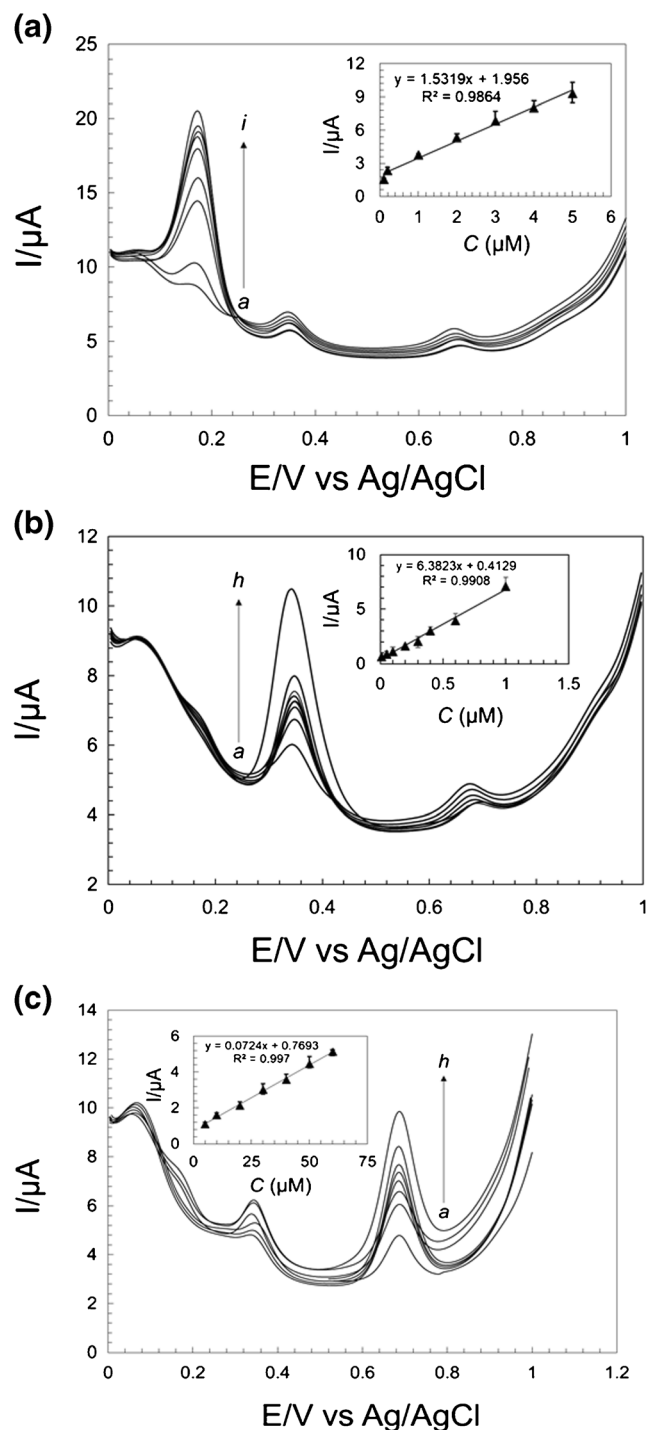the precision of this method. The relative standard deviations (R.S.D.) for each 10 μM DA, 5-HT, and Trp measurements

Fig. 5 DPVs of simultaneous determination of DA, 5-HT, and L-Trp in the presence of AA using GCE/P-Arg/ErGO/AuNP electrode in pH 7.0 phosphate buffer at scan rate of 50 mV s^{-1}. **a** 0.1–5.0 μM of DA (a-i) in the presence of 400 μM AA, 0.5 μM 5-HT, and 5 μM L-Trp; **b** 0.01–1.0 μM of 5-HT (a-h) in the presence of 400 μM AA, 0.1 μM DA, and 5.0 μM L-Trp; **c** 5.0–60 μM of L-Trp (a-h) in the presence of 400 μM AA, 0.1 μM DA, and 0.5 μM 5-HT. The insets show the calibration plot for each analyte ($n = 3$)

Table 2 Simultaneous determination of DA, 5-HT, and L-Trp in human urine samples. ($n = 3$)

Sample	Analyte	Added (μM)	Detected (μM)	Recovery (%)	RSD (%)
Urine 1	DA	0.05	0.049	98.0	1.44
	5-HT	0.1	0.101	101.0	0.86
	L-Trp	0.05	0.05	100.2	1.15
Urine 2	DA	5.0	4.98	99.6	1.37
	5-HT	5.0	5.03	102.6	0.98
	L-Trp	10.0	9.88	98.8	1.67

($n = 10$) were 1.72, 1.23 and 2.87% respectively, indicating an excellent detecting reproducibility. For stability test, the modified electrode was kept at 4 °C for 2 weeks and the peak current did not have an obvious change (lower than 5%) for the same concentration of 10 μM analyte solution, illustrating the good film stability of the sensor.

Since the presence of high concentration of AA in biological systems together with monoamine neurotransmitters, interference study was performed before target analytes determination. From Fig. 5, we observed that AA doesn't interfere with the measurement of DA, 5-HT and L-Trp. The effect of some possible other main interfering substances was also examined. Indeed, it was observed that 100-fold excess L-cysteine, Na^+, K^+, Ca^{2+}, and Zn^{2+}, 300-fold excess glucose, 200-fold excess urea, and 100-fold excess citric acid caused only negligible change and did not interfere with the measurement of the mixer of 10 μM of DA, 5-HT and L-Trp in 0.1 M PB (pH 7.0). Hence, the sensor has good selectivity towards the simultaneous determination of DA, 5-HT, and L-Trp. The relative response of the sensor in the presence of the various examined interferants was shown in the **Table S1**.

Real sample analysis

To investigate the practicality of the method, GCE/P-Arg/ErGO/AuNP electrode was applied to the determination of DA, 5-HT, and L-Trp in healthy human urine using the standard addition method. The human urine samples were diluted 100 times using 0.1 M PB (pH 7.0). The recovery results ranged from 98.0 to 102.6% reveals the possibility of the sensor for real biological samples. Good recovery values were observed and the results are summarized in Table 2.

However, the major limitations of this sensor are the complex modification procedure and operational capabilities. Meanwhile, this technique has limitations in simultaneous multiple analyte detection and sometimes results overlapped voltammetric response.

Conclusion

A novel electrochemical sensor was prepared for the individual and simultaneous determination of DA, 5-HT, and L-Trp

in the presence of ascorbic acid. The GCE/P-Arg/ErGO/AuNP electrode successfully resolved the overlapped voltammetric signals of target analytes into well-separated peaks by the DPV method. In particular, the electrode showed wide linear concentration ranges, very low detection limit and good selectivity. The sensor shows high electrocatalytic activity, efficacy, excellent stability and reproducibility towards the electro-oxidation of DA, 5-HT, and L-Trp. Hence, the prepared GCE/PArg/ ErGO/AuNP sensor provides a potential platform for the analysis of DA, 5-HT, and L-Trp in biological samples for diagnostic research. Despite of some limitations, this sensor may contribute for point-to-care applications. Further extensive studies are suggested on the clinical application and long-term biocompatibility of the electrode.

Compliance with ethical standards   The author(s) declare that they have no competing interests.

References

1. Moccelini SK, Fernandes SC, Vieira IC (2008) Bean sprout peroxidase biosensor based on l-cysteine self-assembled monolayer for the determination of dopamine. Sensors Actuators B Chem 133: 364–369. https://doi.org/10.1016/J.SNB.2008.02.039
2. Lee H, Dellatore SM, Miller WM, Messersmith PB (2007) Mussel-inspired surface chemistry for multifunctional coatings. Science 318:426–430. https://doi.org/10.1126/science.1147241
3. Rand E, Periyakaruppan A, Tanaka Z, Zhang DA, Marsh MP, Andrews RJ, Lee KH, Chen B, Meyyappan M, Koehne JE (2013) A carbon nanofiber based biosensor for simultaneous detection of dopamine and serotonin in the presence of ascorbic acid. Biosens Bioelectron 42:434–438. https://doi.org/10.1016/j.bios.2012.10.080
4. Han HS, Lee HK, You JM, Jeong H, Jeon S (2014) Electrochemical biosensor for simultaneous determination of dopamine and serotonin based on electrochemically reduced GO-porphyrin. Sensors Actuators B Chem 190:886–895. https://doi.org/10.1016/j.snb.2013.09.022
5. Tığ GA (2017) Development of electrochemical sensor for detection of ascorbic acid, dopamine, uric acid and l-tryptophan based on ag nanoparticles and poly(l-arginine)-graphene oxide composite. J

Electroanal Chem 807:19–28. https://doi.org/10.1016/J.JELECHEM.2017.11.008

6. Yokuş ÖA, Kardaş F, Akyildirim O et al (2016) Sensitive voltammetric sensor based on polyoxometalate/reduced graphene oxide nanomaterial: application to the simultaneous determination of l-tyrosine and l-tryptophan. Sensors Actuators B Chem 233:47–54. https://doi.org/10.1016/j.snb.2016.04.050

7. Sun Y, Fei J, Hou J, Zhang Q, Liu Y, Hu B (2009) Simultaneous determination of dopamine and serotonin using a carbon nanotubes-ionic liquid gel modified glassy carbon electrode. Microchim Acta 165:373–379. https://doi.org/10.1007/s00604-009-0147-1

8. Khan ZH, Nakanishi T, Osaka T (2011) Potentiometric detection of serotonin , melatonin , and their precursors / metabolites with monolayer- modified indium tin oxide electrode and their concentration dependency. Sens Lett 9:1849–1852. https://doi.org/10.1166/sl.2011.1739

9. Wang Y, Ouyang X, Ding Y, Liu B, Xu D, Liao L (2016) An electrochemical sensor for determination of tryptophan in the presence of DA based on poly(<scp>l</scp> −methionine)/graphene modified electrode. RSC Adv 6:10662–10669. https://doi.org/10.1039/C5RA24116B

10. Dinesh B, Veeramani V, Chen S-M, Saraswathi R (2017) In situ electrochemical synthesis of reduced graphene oxide-cobalt oxide nanocomposite modified electrode for selective sensing of depression biomarker in the presence of ascorbic acid and dopamine. J Electroanal Chem 786:169–176. https://doi.org/10.1016/J.JELECHEM.2017.01.022

11. Raj M, Gupta P, Goyal RN, Shim Y-B (2017) Graphene/conducting polymer nano-composite loaded screen printed carbon sensor for simultaneous determination of dopamine and 5-hydroxytryptamine. Sensors Actuators B Chem 239:993–1002. https://doi.org/10.1016/J.SNB.2016.08.083

12. Li Y, Li H, Li M, Li C, Sun D, Yang B (2017) Porous boron-doped diamond electrode for detection of dopamine and pyridoxine in human serum. Electrochim Acta 258:744–753. https://doi.org/10.1016/J.ELECTACTA.2017.11.121

13. Ejaz A, Joo Y, Jeon S (2017) Fabrication of 1,4-bis(aminomethyl)benzene and cobalt hydroxide @ graphene oxide for selective detection of dopamine in the presence of ascorbic acid and serotonin. Sensors Actuators B Chem 240:297–307. https://doi.org/10.1016/J.SNB.2016.08.171

14. Wilson TA, Musameh M, Kyratzis IL, Zhang J, Bond AM, Hearn MTW (2017) Enhanced NADH oxidation using Polytyramine/carbon nanotube modified electrodes for ethanol biosensing. Electroanalysis 29:1985–1993. https://doi.org/10.1002/elan.201700146

15. Hasanzadeh M, Mokhtari F, Shadjou N, Eftekhari A, Mokhtarzadeh A, Jouyban-Gharamaleki V, Mahboob S (2017) Poly arginine-graphene quantum dots as a biocompatible and non-toxic nanocomposite: layer-by-layer electrochemical preparation, characterization and non-invasive malondialdehyde sensory application in exhaled breath condensate. Mater Sci Eng C 75:247–258. https://doi.org/10.1016/j.msec.2017.02.025

16. Yi Y, Zhu G, Wu X, Wang K (2016) Highly sensitive and simultaneous electrochemical determination of 2-aminophenol and 4-aminophenol based on poly(l-arginine)-β-cyclodextrin/carbon nanotubes@graphene nanoribbons modified electrode. Biosens Bioelectron 77:353–358. https://doi.org/10.1016/j.bios.2015.09.052

17. Zhou X, Jing W, Zhuang Z, Zheng X (2015) In situ synthesis of gold nanoparticles on poly (L-arginine) modified glassy carbon electrode and Electrocatalytic oxidation of glucose in alkaline solution. ECS Electrochem Lett 4:G5–G7. https://doi.org/10.1149/2.0071508eel

18. Devadas B, Cheemalapati S, Chen SM, Ali MA, al-Hemaid FMA (2014) Highly sensing graphene oxide/poly-arginine-modified electrode for the simultaneous electrochemical determination of buspirone, isoniazid and pyrazinamide drugs. Ionics (Kiel) 21:547–555. https://doi.org/10.1007/s11581-014-1179-z

19. Khan MZH (2017) Nanoparticles modified ITO based biosensor. J Electron Mater 46:2254–2268. https://doi.org/10.1007/s11664-016-5172-3

20. Khan MZH (2017) Graphene oxide modified electrodes for dopamine sensing. J Nanomater 2017:1–11. https://doi.org/10.1155/2017/8178314

21. Mishra SK, Srivastava AK, Kumar D, Biradar AM, Rajesh (2013) Microstructural and electrochemical impedance characterization of bio-functionalized ultrafine ZnS nanocrystals–reduced graphene oxide hybrid for immunosensor applications. Nanoscale 5:10494. https://doi.org/10.1039/c3nr02575f

22. Moozarm Nia P, Woi PM, Alias Y (2017) Facile one-step electrochemical deposition of copper nanoparticles and reduced graphene oxide as nonenzymatic hydrogen peroxide sensor. Appl Surf Sci 413:56–65. https://doi.org/10.1016/j.apsusc.2017.04.043

23. Weng H, Liao F, Wang M, Lin M, Ge X (2016) One-pot synthesis of porous au-nanoparticles@polymer/reduced graphene oxide composite microspheres by γ-ray radiation and their application as a recyclable high-performance catalyst. RSC Adv 6:59684–59691. https://doi.org/10.1039/C6RA11205F

24. Otari SV, Kumar M, Anwar MZ, Thorat ND, Patel SKS, Lee D, Lee JH, Lee JK, Kang YC, Zhang L (2017) Rapid synthesis and decoration of reduced graphene oxide with gold nanoparticles by thermostable peptides for memory device and photothermal applications. Sci Rep 7:10980. https://doi.org/10.1038/s41598-017-10777-1

25. Huang J, Zhang L, Chen B, Ji N, Chen F, Zhang Y, Zhang Z (2010) Nanocomposites of size-controlled gold nanoparticles and graphene oxide: formation and applications in SERS and catalysis. Nanoscale 2:2733. https://doi.org/10.1039/c0nr00473a

26. Morioku K, Morimoto N, Takeuchi Y, Nishina Y (2016) Concurrent formation of carbon–carbon bonds and functionalized graphene by oxidative carbon-hydrogen coupling reaction. Sci Rep 6:25824. https://doi.org/10.1038/srep25824

27. Khan MZH, Shahed SMF, Yuta N, Komeda T (2017) Deposition of an Ultraflat graphene oxide Nanosheet on atomically flat substrates. J Electron Mater 46:4160. https://doi.org/10.1007/s11664-017-5327-x

28. Du J, Yue R, Ren F et al (2014) Novel graphene flowers modified carbon fibers for simultaneous determination of ascorbic acid, dopamine and uric acid. Biosens Bioelectron 53:220–224. https://doi.org/10.1016/J.BIOS.2013.09.064

29. Sun D, Li H, Li M, Li C, Dai H, Sun D, Yang B (2018) Electrodeposition synthesis of a NiO/CNT/PEDOT composite for simultaneous detection of dopamine, serotonin, and tryptophan. Sensors Actuators B Chem 259:433–442. https://doi.org/10.1016/J.SNB.2017.12.037

30. Ghoreishi SM, Behpour M, Ghoreishi FS, Mousavi S (2017) Voltammetric determination of tryptophan in the presence of uric acid and dopamine using carbon paste electrode modified with multi-walled carbon nanotubes. Arab J Chem 10:S1546–S1552. https://doi.org/10.1016/J.ARABJC.2013.05.016

31. Liu B, Ouyang X, Ding Y, Luo L, Xu D, Ning Y (2016) Electrochemical preparation of nickel and copper oxides-decorated graphene composite for simultaneous determination of dopamine, acetaminophen and tryptophan. Talanta 146:114–121. https://doi.org/10.1016/J.TALANTA.2015.08.034

32. Zhuang X, Chen D, Zhang S, et al (2018) Reduced graphene oxide functionalized with a CoS 2 / ionic liquid composite and decorated with gold nanoparticles for voltammetric sensing of dopamine. 2:

33. Yao Z, Yang X, Niu Y, Wu F, Hu Y, Yang Y (2017) Voltammetric dopamine sensor based on a gold electrode modified with reduced graphene oxide and Mn3O4 on gold nanoparticles. Microchim Acta 184:2081–2088. https://doi.org/10.1007/s00604-017-2210-7

34. Liu J, Xie Y, Wang K, Zeng Q, Liu R, Liu X (2017) A nanocomposite consisting of carbon nanotubes and gold nanoparticles in an amphiphilic copolymer for voltammetric determination of dopamine, paracetamol and uric acid. Microchim Acta 184:1739–1745. https://doi.org/10.1007/s00604-017-2185-4

35. Chen J, He P, Bai H, He S, Zhang T, Zhang X, Dong F (2017) Poly(β-cyclodextrin)/carbon quantum dots modified glassy carbon electrode: preparation, characterization and simultaneous electrochemical determination of dopamine, uric acid and tryptophan. Sensors Actuators B Chem 252:9–16. https://doi.org/10.1016/J.SNB.2017.05.096

36. Wang S, Wang Y, Min Q et al (2016) Simultaneous electrochemical determination of dopamine and serotonin in rat cerebrospinal fluid using screen-printed electrode modified with MWNTs-SiO 2 - chitosan composites. Int J Electrochem Sci 11:2360–2376

37. Kaur B, Satpati B, Srivastava R (2015) Synthesis of NiCo $_2$ O $_4$ /Nano-ZSM-5 nanocomposite material with enhanced electrochemical properties for the simultaneous determination of ascorbic acid, dopamine, uric acid and tryptophan. New J Chem 39:1115–1124. https://doi.org/10.1039/C4NJ01360C

38. Narouei FH, Tammandani HK, Ghalandarzehi Y et al (2017) An electrochemical sensor based on conductive polymers/graphite paste electrode for simultaneous determination of dopamine, uric acid and tryptophan in biological samples. Int J Electrochem Sci 12:7739–7753. https://doi.org/10.20964/2017.08.50